

Contribution to the supersolid JLTP special issue SS2012

# Classification of a supersolid: Symmetry breaking and Excitation spectra

Yu Chen <sup>1</sup>, Jinwu Ye<sup>2,3</sup> and Quang Shan Tian <sup>1</sup>

<sup>1</sup>*Department of Physics, Peking University, Beijing 100871, China*

<sup>2</sup> *Department of Physics and Astronomy, Mississippi State University, P. O. Box 5167, Mississippi State, MS, 39762*

<sup>3</sup> *Department of Physics, Capital Normal University, Beijing, 100048 China*

(Dated: November 1, 2019)

A state of matter is characterized by its symmetry breaking and elementary excitations. A supersolid is a state which breaks both translational symmetry and internal  $U(1)$  symmetry. Here, we review some recent works and also provide additional new insights in studying symmetry breaking and the excitation spectra of various kinds supersliods in both continuous systems and on lattices, both condensed matter and cold atom systems. Our approaches are from both phenomenological Ginsburg-Landau theory and microscopic numerical calculations, We also contrast different kinds of supersolids in term of its order parameters, symmetry breaking patterns, excitation spectra and detection methods.

## I. INTRODUCTION

A solid can not flow. It breaks a continuous translational symmetry into a discrete lattice translational symmetry. There are low energy lattice phonon excitations in the solid. While a superfluid can flow even through narrowest channels without any resistance. It breaks a global  $U(1)$  symmetry and has the off-diagonal long range order (ODLRO). There are low energy superfluid phonon excitations in the superfluid. A supersolid is a state which breaks both the continuous translational symmetry and the global  $U(1)$  symmetry, therefore has both the crystalline order and the ODLRO. The possibility of a supersolid phase in  $^4He$  was theoretically speculated in 1970<sup>1</sup>. Over the last 40 years, a number of experiments have been designed to search for the supersolid state. Most notably, by using torsional oscillator measurements, the PSU group lead by Chan observed a marked  $1 \sim 2\%$  NCRI of solid  $^4He$  at  $\sim 0.2K$  in bulk  $^4He$ <sup>2</sup>. The authors suggested that the supersolid state of  $^4He$  maybe responsible for the NCRI. The PSU experiments rekindled extensive both experimental<sup>3-8</sup> and theoretical<sup>9-17</sup> interests. So far, there is still a controversy if a supersolid phase indeed exist in  $^4He$  system and is responsible for the NCRI observed in the PSU experiments.

No matter if supersolid indeed exists in the  $^4He$  system or not, it is a new state of matter which will display its own characteristic behaviors not shared by any other states of matter. In this short paper, instead of trying to resolve this controversy, we will discuss very general properties of a supersolid such as its symmetry breaking, elementary excitation spectra and detections in various possible experimental systems. It may also be realized in other various bosonic or fermionic, continuous or optical lattice systems.

The rest of the paper is organized as following. Sect. II is dedicated to supersolids in continuous 3d and 2d systems. We review the elementary excitation spectrum ( called

supersolidon ) in a possible 3d  $^4He$  supersolid with Van der Walls interaction in Sec.I-A, then discuss a possible exciton supersolid with dipole-dipole interaction in a 2d electron-hole bilayer system in some intermediate distances. Sect. III is dedicated to supersolids in lattice systems. We stress some analogy and also important differences between the continuous supersolids and lattice supersolids such as excitation spectrum, detection methods, new kinds of supersolids special to a lattice system and so on. Sect. IV is dedicated to the excitation spectrum in an superfluid density wave in a continuous system, namely, an inhomogeneous superfluid. Sect. V is dedicated to a  $Z_2$  superfluid density wave in an optical cavity which was already realized in experiments with cold atoms inside a high-fineness transverse pumping optical cavity. In the final Sec.VI, we summarize our main results and also contrast different kinds of supersolids addressed in this paper.

## II. SUPERSOLIDS IN CONTINUOUS SYSTEMS

In this section, we review some previous work on supersolids in 3 dimensional  $^4He$  system and possible exciton supersolids in 2 dimensional electron-hole bilayer systems. Both can be classified as supersolids in continuous systems. The phenomenological Ginsburg-landau theory was written down for both systems. The main purposes for the GL theory is (1) At the mean field level, the GL theory can be used to determine the lattice structure of a supersolid, (2) When considering fluctuations above the mean field solutions, one may study transitions among different phases. (3) Well inside a given phase, especially inside a supersolid, one can study the elementary excitations inside such a given phase.

Classical non-equilibrium hydrodynamics inside a SS was investigated for a long time<sup>1</sup>. These hydrodynamics will break down at very low temperature where quantum fluctuations dominate. The quantum nature of the excitations in a SS was studied in<sup>14,15</sup>. The phonon spectrum in a solid and the superfluid phonon ( or Goldstone mode ) in a superfluid have all been detected by inelastic neutron scattering experiments. So detecting these "supersolidons" by possible inelastic neutron scattering experiments or acoustic attenuation experiments could be smoking gun experiments to confirm a supersolid in any continuous systems. Because the excitation spectra of a SS is one of the most important characteristics of a supersolid, here, we will review only the quantum characteristics of low energy excitations in the SS, namely, focus on the (3) in the above. We refer (1) and (2) to the original papers.

### A. Possible supersolid in $^4He$ with Van der Waals force.

Well inside the SS, the translational symmetry is already broken, so we can parameterize the density deviation order parameter  $\delta n(\vec{x}, \tau) = n(\vec{x}, \tau) - n_0$  and the SF complex order parameter  $\psi(\vec{x}, \tau)$  as:

$$\begin{aligned} \delta n(\vec{x}, \tau) &= \sum_{\vec{G}}' n_{\vec{G}} e^{i\vec{G} \cdot (\vec{x} + \vec{u}(\vec{x}, \tau))} \\ \psi(\vec{x}, \tau) &= \psi_0(\vec{x}, \tau) [1 \pm \frac{1}{P} \sum_{\vec{G}}' e^{i\vec{G} \cdot (\vec{x} + \vec{u}(\vec{x}, \tau))}] \end{aligned} \quad (1)$$

where the  $\psi_0(\vec{x}, \tau) = |\psi_0(\vec{x}, \tau)|e^{i\theta(\vec{x}, \tau)}$  is the SF order parameter,  $\vec{u}(\vec{x}, \tau)$  are the 3 lattice phonon modes, the  $\pm$  means vacancy-type or interstitial-type supersolids respectively,  $n_{\vec{G}}^* = n_{-\vec{G}}$  the " / " means the sum over the shortest non-zero reciprocal lattice vector  $\vec{G}$  and  $P$  is the number of them.

The long wavelength effective action describing the low energy modes inside the SS phase was derived in<sup>14,15</sup>:

$$\mathcal{L} = \frac{1}{2}[\kappa(\partial_\tau\theta)^2 + \rho_{\alpha\beta}^s\partial_\alpha\theta\partial_\beta\theta] + \frac{1}{2}[\rho_n(\partial_\tau u_\alpha)^2 + \lambda_{\alpha\beta\gamma\delta}u_{\alpha\beta}u_{\gamma\delta}] + a_{\alpha\beta}u_{\alpha\beta}i\partial_\tau\theta \quad (2)$$

where  $\kappa$  is the SF compressibility and  $\rho_{\alpha\beta}^s$  is the SF stiffness which has the same symmetry as  $a_{\alpha\beta}$ . The  $\rho_n$  is the normal density, the  $\lambda_{\alpha\beta\gamma\delta}$  is the stress tensor. Obviously, the last term is the crucial *Berry phase* coupling term which couples the lattice phonon modes to the SF mode. The factor of  $i$  is important in this coupling. By integration by parts, this term can also be written as  $a_{\alpha\beta}(\partial_\tau u_\beta\partial_\alpha\theta + \partial_\tau u_\alpha\partial_\beta\theta)$  which has the clear physical meaning of the coupling between the SF velocity  $\partial_\alpha\theta$  and the velocity of the lattice vibration  $\partial_\tau u_\beta$ . It is this term which makes the low energy modes in the SS to have its own characteristics which could be detected by experiments. The invariance under the Galilean transformation<sup>17</sup> dictates that  $a_{\alpha\beta} = \rho_n\delta_{\alpha\beta} - \rho_{\alpha\beta}^s$ . Here, we only review the isotropic solid case, the *hcp* lattice and the effects of the topological vortex loop excitations were discussed in the original papers<sup>14,15</sup>.

A truly isotropic solid can only be realized in a highly poly-crystalline sample. Usual samples are not completely isotropic. However, we expect the simple physics brought about in an isotropic solid may also apply qualitatively to other samples which is very poly-crystalline. For an isotropic solid,  $\lambda_{\alpha\beta\gamma\delta} = \lambda\delta_{\alpha\beta}\delta_{\gamma\delta} + \mu(\delta_{\alpha\gamma}\delta_{\beta\delta} + \delta_{\alpha\delta}\delta_{\beta\gamma})$  where  $\lambda$  and  $\mu$  are Lame coefficients,  $\rho_{\alpha\beta}^s = \rho^s\delta_{\alpha\beta}$ ,  $a_{\alpha\beta} = a\delta_{\alpha\beta}$  where  $a = \rho_n - \rho_s$ . In  $(\vec{q}, \omega_n)$  space, Eqn.2 becomes:

$$\begin{aligned} \mathcal{L}_{is} = & \frac{1}{2}[\rho_n\omega_n^2 + (\lambda + 2\mu)q^2]|u_l(\vec{q}, \omega_n)|^2 + \frac{1}{2}[\kappa\omega_n^2 + \rho_sq^2]|\theta(\vec{q}, \omega_n)|^2 \\ & + aq\omega_nu_l(-\vec{q}, -\omega_n)\theta(\vec{q}, \omega_n) + \frac{1}{2}[\rho_n\omega_n^2 + \mu q^2]|u_t(\vec{q}, \omega_n)|^2 \end{aligned} \quad (3)$$

where  $u_l(\vec{q}, \omega_n) = iq_iu_i(\vec{q}, \omega_n)/q$  is the longitudinal component,  $u_t(\vec{q}, \omega_n) = i\epsilon_{ij}q_iu_j(\vec{q}, \omega_n)/q$  are transverse components of the displacement field. Note that Eqn.3 shows that only longitudinal component couples to the superfluid  $\theta$  mode, while the two transverse components are unaffected by the superfluid mode. This is expected, because the superfluid mode is a longitudinal density mode itself which does not couple to the transverse modes.

From Eqn.3, we can identify the longitudinal-longitudinal phonon correlation function:

$$\langle u_l u_l \rangle = \frac{\kappa\omega_n^2 + \rho_sq^2}{(\kappa\omega_n^2 + \rho_sq^2)(\rho_n\omega_n^2 + (\lambda + 2\mu)q^2) + a^2q^2\omega_n^2} \quad (4)$$

The  $\langle \theta\theta \rangle$  and  $\langle u_l\theta \rangle$  correlation functions can be similarly written down. By doing the analytical continuation  $i\omega_n \rightarrow \omega + i\delta$ , we can identify the two poles of all the correlation functions at  $\omega_\pm^2 = v_\pm^2q^2$ ,  $q \ll G$  where the two velocities  $v_\pm$  is given by:

$$v_\pm^2 = [\kappa(\lambda + 2\mu) + \rho_s\rho_n + a^2 \pm \sqrt{(\kappa(\lambda + 2\mu) + \rho_s\rho_n + a^2)^2 - 4\kappa\rho_s\rho_n(\lambda + 2\mu)}]/2\kappa\rho_n \quad (5)$$

If setting  $a = 0$ , then  $v_\pm^2$  reduces to the longitudinal phonon velocity  $v_{lp}^2 = (\lambda + 2\mu)/\rho_n$  and the superfluid velocity  $v_s^2 = \rho_s/\kappa$  respectively. Of course, the transverse phonon velocity

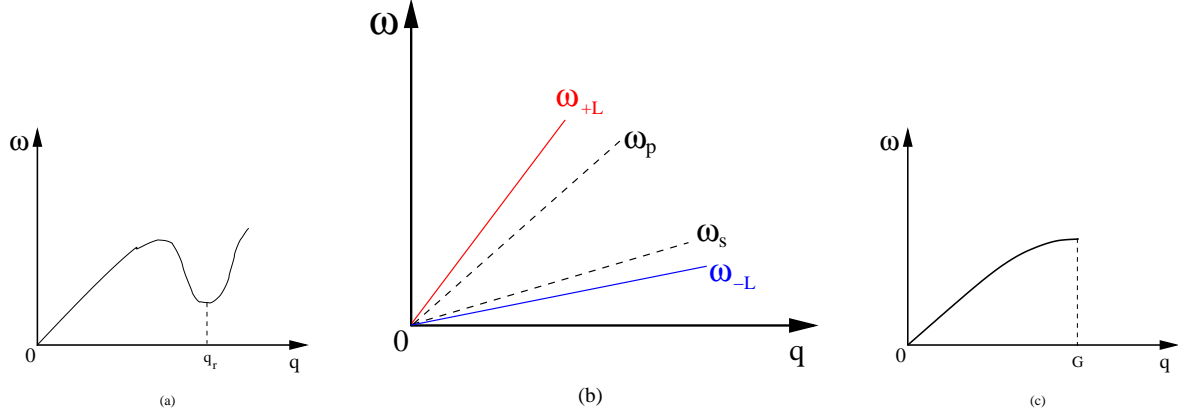


FIG. 1: The elementary low energy excitations inside a (a) superfluid (b) supersolid (c) solid. For simplicity, only excitation spectra in a simplified 3d isotropic solid and 2d triangular lattice were shown. In (b) The coupling between the phonon mode  $\omega_p = v_p q$  ( the upper dashed line ) and the superfluid mode  $\omega_s = v_s q$  ( the lower dashed line ) leads to the two new "supersolidon" modes  $\omega_{\pm} = v_{\pm} q$ ,  $q \ll G$  ( solid lines ) in the SS. Their corresponding spectral weights are listed in Eqn.6 and 7. These two new supersolid modes and the spectral weights should be detected by in-elastic neutron scatterings.

$v_{tp}^2 = \mu/\rho_n$  is untouched. For notation simplicity, in the following, we just use  $v_p$  for  $v_{lp}$ . Inside the SS, due to the very small superfluid density  $\rho_s$ , it is expected that  $v_p > v_s$ . In fact, in isotropic solid  $He^4$ , it was measured that  $v_{lp} \sim 450 - 500 m/s$ ,  $v_t \sim 230 \sim 320 m/s$  and  $v_s \sim 366 m/s$  near the melting curve<sup>6</sup>. It is easy to show that  $v_+ > v_p > v_s > v_-$  and  $v_+^2 + v_-^2 > v_p^2 + v_s^2$ , but  $v_+ v_- = v_p v_s$ , so  $v_+ + v_- > v_p + v_s$  ( see Fig.1 ). Note that because the Galilean invariance dictates  $a = \rho_n - \rho_s$ , for  $\rho_s \ll \rho_n$ , one can see  $\rho_s \rho_n + a^2 \gg \rho_s \rho_n$ , so  $v_+$  ( $v_-$ ) are considerably above ( below )  $v_p$  ( $v_s$ ), so the two supersolidons, especially the softening of the lower branch, may be easily distinguished by possible neutron scattering experiments.

By doing the analytical continuation  $i\omega_n \rightarrow \omega + i\delta$ , we can take the imaginary part and find:

$$\begin{aligned} Im \langle u_l u_l \rangle_{i\omega_n \rightarrow \omega + i\delta} &= \frac{v_s^2 - v_+^2}{v_+^2 - v_-^2} \frac{\pi}{2\rho_n v_+ q} \frac{1}{q} [\delta(\omega - v_+ q) - \delta(\omega + v_+ q)] \\ &\quad - \frac{v_s^2 - v_-^2}{v_+^2 - v_-^2} \frac{\pi}{2\rho_n v_- q} \frac{1}{q} [\delta(\omega - v_- q) - \delta(\omega + v_- q)] \end{aligned} \quad (6)$$

It is easy to see that the second term can be achieved from the first term just by  $v_+ \leftrightarrow v_-$ . Setting  $a = 0$ , then  $v_+ = v_p$ ,  $v_- = v_s$ , the second term just vanishes, the first term recovers the excitation spectrum of the lattice phonons. When  $a \neq 0$ , then Eqn.6 becomes a mixing of the lattice phonons and superfluid phonons, the first and second term give the excitation energies and the two corresponding spectral weights.

Very similarly, we can find

$$\begin{aligned} Im\langle\theta\theta\rangle_{i\omega_n \rightarrow \omega+i\delta} &= \frac{v_p^2 - v_+^2}{v_+^2 - v_-^2} \frac{\pi}{2\kappa v_+} \frac{1}{q} [\delta(\omega - v_+q) - \delta(\omega + v_+q)] \\ &- \frac{v_p^2 - v_-^2}{v_+^2 - v_-^2} \frac{\pi}{2\kappa v_-} \frac{1}{q} [\delta(\omega - v_-q) - \delta(\omega + v_-q)] \end{aligned} \quad (7)$$

It is easy to see that the second term can be achieved from the first term just by  $v_+ \leftrightarrow v_-$ . Setting  $a = 0$ , then  $v_+ = v_p$ ,  $v_- = v_s$ , the first term just vanishes, the second term recovers the excitation spectrum of the superfluid phonons. When  $a \neq 0$ , then Eqn.7 become a mixing of the lattice phonons and superfluid phonons, the first and second term give the excitation energies and the two corresponding spectral weights. So detecting these "supersolidons" in Fig.1b by possible inelastic neutron scattering experiments or acoustic attenuation experiments could be smoking gun experiments to confirm a supersolid in any continuous systems.

However, it is well known that the GL theory is a phenomenological theory. In fact, depending on the parameter regimes in the GL theory in<sup>15</sup>, the author discussed both the non-existence and existence of supersolid, also the vacancy-type and interstitial-type the supersolid if it exists. Into which parameter regime will the <sup>4</sup>He fall can only be studied by various numerical calculations<sup>9,10</sup>. But so far, it seems that most of the numerical simulations with the <sup>4</sup>He atoms interacting each other with Van der Waals forces favor a commensurate solid instead of either vacancy-type or interstitial type supersolid. Even so, the supersolid could be a meat-stable phase with sufficiently long life time and lead to some experimental observable signatures within some time scale.

## B. Possible Exciton supersolid in electron-hole bilayer with dipole-dipole interaction.

In this subsection, we will discuss another bosonic system with much longer range dipole-dipole interactions: excitons in electron-hole semi-conductor bilayer (EHBL) systems<sup>18</sup>. We will argue this system may have a better chance to realize a supersolid in some parameter regime. There are also some numerical evidences to support such a claim<sup>36</sup>.

In the last decade, degenerate exciton systems have been produced by different experimental groups with different methods in quasi-two-dimensional semiconductor *GaAs/AlGaAs* coupled quantum wells structure<sup>18</sup>. There are two important dimensionless parameters in the EHBL. (1) One is the dimensionless distance  $\gamma = d/a_{ex}$  between the two layers. The  $a_{ex} = \hbar^2\epsilon/e^2m_r = \epsilon \frac{m_0}{m_r} a_B \sim 100a_B \sim 50\text{\AA}$  is the size of an exciton, the  $m_0$  is the electron bare mass and  $1/m_r = 1/m_e + 1/m_h$  is the reduced mass of the excitons and  $a_B = \hbar^2/e^2m_0 \sim 0.53\text{\AA}$  is the bare Bohr radius. The binding energy of an exciton is  $E_b = -e^2/2a_{ex}\epsilon = -\frac{m_r}{m_0} \frac{1}{\epsilon^2} \frac{e^2}{2a_B} \sim -10\text{meV}$ . (2) Another is  $r_s$ . The  $r_s a_{ex}$ , defined by  $\pi(r_s a_{ex})^2 n = 1$ , is the typical interparticle distance in a single layer. The  $r_s$  is the ratio of the potential energy over kinetic energy in a single layer. It is easy to see that the ratio of intralayer Coulomb  $V_{11}$  over the interlayer Coulomb  $V_{12}$  interaction is given by  $\alpha = V_{11}/V_{12} = d/r_s a_{ex}$ . So when the interlayer Coulomb interaction dominates  $\alpha < 1$ , the EHBL is expected to exhibit the superfluid of excitons. If the density of excitons is sufficiently low ( large  $r_s$  ), then the system is in a weakly coupled Wigner solid state at very large distance and become an BEC excitonic superfluid ( ESF ) at short distance. In

the following, we argue<sup>18</sup> that there could be an exciton supersolid (ESS) phase intervening between the ESF and Wigner solid phase, as the system evolves from the BEC ESF to the weakly coupled Wigner solid when the distance increases. The argument relies heavily on the dipole-dipole interaction between the excitons.

If we assume an exciton is already formed at relatively short interlayer distance, its kinetic energy  $K \sim \frac{\hbar^2}{M(r_s a_{ex})^2}$  where  $M = m_e + m_h$  is the total mass of an exciton. Due to the dipole-dipole interactions between the excitons, its potential energy  $P \sim \frac{e^2 d^2}{\epsilon (r_s a_{ex})^3}$ . When  $K < P$ , namely,  $\sqrt{m_r/M} \sqrt{r_s} < d/a_{ex}$ , the EHBL could favor a excitonic ( or dipolar ) normal solid (ENS) state. As argued above, when  $d/a_{ex} < r_s$ , the EHBL is in a ESF state. So in the intermediate distance  $\sqrt{r_s}/2 < d/a_{ex} < r_s$  where we used  $M/m_r \sim 5$ , the system may favor a excitonic ( or dipolar ) supersolid (ESS) state. When  $d/a_{ex} > r_s$ , it will become the excitonic normal solid (ENS) due to the long range dipole-dipole  $1/r^3$  repulsive interactions. For the present experimental density regime<sup>18</sup>  $n \sim 10^{10} \text{ cm}^{-2}$ ,  $r_s \sim 20$ , so the excitons are tightly bound pairs in real space. In this  $r_s \sim 20 \gg 1$  limit, there is a broad distance regime  $2 < d/a_{ex} < 20$  where the system could be in the ESS state. As the distance increases to the critical distance  $d > d_{c1}$ , the roton minimum in the Fig.1a may drive the instability of the ESF to a formation of a solid. Because the lattice constant  $r_s a_{ex}$  of the resulting solid is completely fixed by the parameter  $r_s$  which is independent of the distance, so the resulting solid is likely to have vacancies with density  $n_v(0)$  even at  $T = 0$ . By contrast, in solid Helium 4, the density is self-determined by the pressure  $n = \frac{\partial P}{\partial \mu}|_{T,V}$ , so the density and pressure go hand in hand, the solid  ${}^4\text{He}$  is likely to be commensurate. We expect that the vacancy-vacancy interaction is also a repulsive dipole-dipole one. The condensation of these repulsively interacting vacancies at  $T = 0$  leads to the SF mode inside the in-commensurate ENS. This resulting state is the ESS state with a lattice constant slightly smaller than  $r_s a_{ex}$  to accommodate the extra vacancies. As the distance increases to  $d > d_{c2} > d_{c1}$ ,  $n_v(0) = 0$ , the resulting state is a commensurate ENS whose lattice constant is locked at  $r_s a_{ex}$ . As distance increases further, the ENS will crossover to the two weakly coupled Wigner crystal. It becomes feasible to experimentally explore all the possible phases and phase transitions in the EHBL in the near future.

From the mean field analysis of the Ginsburg-Landau action in<sup>18</sup>, the lattice structure of the excitonic supersolid should be a triangular lattice. When studying the excitations spectrum inside the ESS, a similar GL action can be constructed as its 3 dimensional counter part<sup>18</sup>. For a triangular lattice,  $\lambda_{\alpha\beta\gamma\delta} = \lambda\delta_{\alpha\beta}\delta_{\gamma\delta} + \mu(\delta_{\alpha\gamma}\delta_{\beta\delta} + \delta_{\alpha\delta}\delta_{\beta\gamma})$  where  $\lambda$  and  $\mu$  are Lame coefficients,  $\rho_{\alpha,\beta}^s = \rho^s \delta_{\alpha,\beta}$ ,  $a_{\alpha,\beta} = a\delta_{\alpha,\beta}$ . Eqn.3, the following equations an Fig.1 apply. Note that the isotropic 3d solid discussed in Sec.II-1 is just a simplification. The supersolidons in 3d hcp crystal were discussed in<sup>14</sup>. While Eqn.3 holds rigorously for a 2d triangular lattice. The differences between 3d and 2d cases were discussed in<sup>18</sup>.

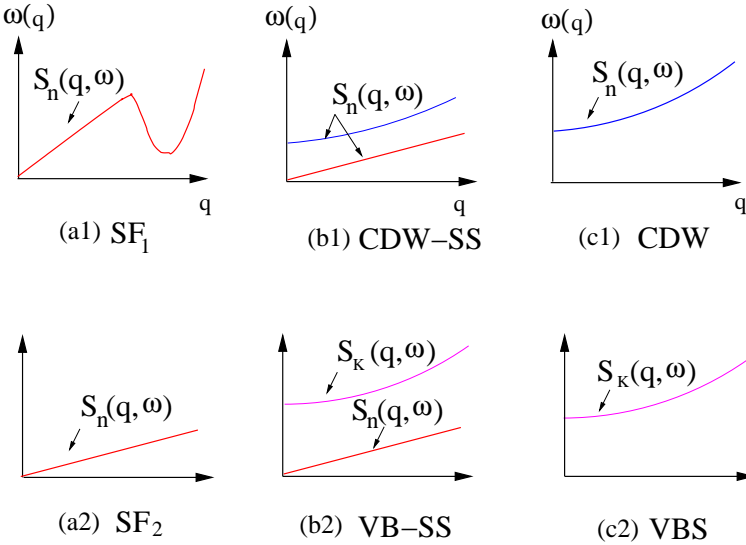


FIG. 2: The excitation spectra in the CDW, VBS, SF, CDW-SS and VB-SS states in a lattice. They correspond to the peak positions of the corresponding dynamic response functions shown with arrows<sup>39</sup>. In the (b1) and (c1) cases, the starting wavevector is  $\vec{Q}_n$  in the upper CDW branch. In the (b2) and (c2) cases, the starting wavevector is  $\vec{Q}_K$  in the upper VBS branch. The corresponding spectral weights are worked out in<sup>39</sup>.

### III. DENSITY WAVE AND VALENCE BOND SUPERSOLIDS IN LATTICE SYSTEMS

The extended boson Hubbard model ( EBHM ) with various kinds of interactions, on all kinds of lattices and at different filling factors is described by the following Hamiltonian:

$$\begin{aligned}
 H = & -t \sum_{\langle ij \rangle} (b_i^\dagger b_j + h.c.) - \mu \sum_i n_i + \frac{U}{2} \sum_i n_i(n_i - 1) \\
 & + V_1 \sum_{\langle ij \rangle} n_i n_j + V_2 \sum_{\langle\langle ik \rangle\rangle} n_i n_k + \dots
 \end{aligned} \tag{8}$$

where  $n_i = b_i^\dagger b_i$  is the boson density,  $t$  is the nearest neighbor hopping amplitude.  $U, V_1, V_2$  are onsite, nearest neighbor (nn) and next nearest neighbor (nnn) interactions respectively, the  $\dots$  may include further neighbor interactions, dipole-dipole interaction  $V_d = \frac{p^2}{|\vec{r}_i - \vec{r}_j|^3}$  and possible ring-exchange interactions. A supersolid in Eqn.8 is defined as the simultaneous orderings of ferromagnet in the  $XY$  component ( namely,  $\langle b_i \rangle \neq 0$  ) and CDW in the  $Z$  component. The EBHM, especially the stability of the supersolid phase has been studied by spin wave expansion<sup>26</sup>, the Quantum Monte-Carlo (QMC) simulations<sup>27-32</sup> and the dual vortex method (DVM)<sup>19-23</sup> which is a GL action in the dual vortex picture.

#### 1. The Dual GL approach: the DVM to study supersolids in lattices

In<sup>21</sup>, based on the dual vortex degree of freedoms<sup>19</sup>, the author developed a systematic dual GL action to study all the possible phases and phase transitions in the EBHM Eqn.8 in bipartite lattices such as a honeycomb and square lattice near half filling. The dual GL theory can be used to derive the symmetry breaking patterns of various insulating and

supersolid states, the transitions among different phases and excitation spectrum in a given insulating phase, especially in various kinds of supersolids. In the insulating side, it was found that there are two consecutive transitions at zero temperature driven by the chemical potential: in the Ising limit, a Commensurate-Charge Density Wave (CDW) at half filling to a narrow window of CDW supersolid (CDW-SS), then to an Incommensurate-CDW ; in the easy-plane limit, a Commensurate-Valence Bond Solid (VBS) at half filling to a narrow window of VBS supersolid ( VB-SS), then to an Incommensurate-VBS. The first transition is second order in the same universality class as the Mott to insulator transition, therefore has the exact critical exponents  $z = 2, \nu = 1/2, \eta = 0$  with logarithmic corrections<sup>25</sup>, while the second one is first order. The VB-SS is a new kind of solid which only happens on a lattice, so no analog in a continuous system discussed in the Sec.II. The VB-SS maybe stabilized in the presence of ring-exchange terms<sup>24</sup>. The excitation spectra in these phases are shown in the Fig.2. The transition from the SF to the CDW-SS transition is driven by the condensation of diagonal vortex-antivortex pair without the condensations of the individual vortex<sup>25</sup>. In the direct boson picture, it may correspond to the gap closing at the roton minimum. The transition from the SF to the VB-SS transition is driven by the condensation of off-diagonal vortex-antivortex pair without the condensations of the individual vortex. Unfortunately, it is still not clear what kind of physical processes it corresponds to in the direct boson picture<sup>25</sup>. Very recently, the author in<sup>22,23</sup> also studied various kinds of supersolids in frustrated lattices such as triangular and Kagome lattices . As first discovered in<sup>26</sup>, a CDW supersolid is very robust in a triangular lattice slightly away the 1/3 filling. It could be either vacancy-like or interstitial-like supersolid. But there is no VB-SS which was discovered in bi-partite lattices. There could also be a CDW-VS supersolid which has the three kinds of orders: CDW-order, VB order and the superfluid order. In a Kagome lattice, there is no VB-SS either, but there could be CDW-SS and the CDW-VB-SS. So the VB-SS is unique to bi-partite lattices, while the CDW-VB-SS is unique to frustrated lattices. While, the CDW-SS can happen in both bi-partite and frustrated lattices.

Just like the GL approach to the possible supersolids in continuous systems discussed in Sec.I, the DVM developed in<sup>19-23</sup> is a symmetry-based approach which, in principle, can be used to classify all the possible phases, especially supersolid phases, and phase transitions. But if a particular phase identified by the DVM will become a stable ground state or not depends on the specific competitions among all the possible parameters in the EBHM in Eqn.8. This kind of question can only be addressed by a microscopic approach such as Quantum Monte-Carlo (QMC) simulations on a specific Hamiltonian. In the following, we just compare with QMC simulations in  $V_1, V_2$  models and the dipole-dipole interaction model  $V_d = \frac{p^2}{|\vec{r}_i - \vec{r}_j|^3}$ .

## 2. QMC simulations in lattices with $V_1, V_2$ interactions

There have been extensive QMC on the EBHM Eqn.8, to especially search for stable supersolid phases in various bipartite and frustrated lattices<sup>27-32</sup>. For hard core bosons in a square lattice, it was shown by the QMC in<sup>27</sup> that the  $(\pi, \pi)$  X-CDW SS slightly away from 1/2 filling is not stable against phase separation with  $U = \infty, V_1 > 0, V_2 = 0$ , but the  $(\pi, 0)$  stripe SS is indeed stable with  $U = \infty, V_1 = 0, V_2 > 0$ . The transition from the stripe SS to the SF is a first order transition<sup>25</sup>. For soft core bosons with  $U < \infty, V_1 > 0, V_2 = 0$ , the interstitial-like supersolid slightly above 1/2 filling is stable, although the vacancy-like supersolid slightly below 1/2 filling is still unstable against phase separation<sup>28</sup>. Similar phenomena were also found for soft core bosons in a honeycomb lattice near half fillings<sup>29</sup>. The claim that the CDW to the CDW-SS transition at  $d = 2$  driven by the

chemical potential is in the same universality class of SF to Mott transition with the critical exponents  $z = 2, \nu = 1/2, \eta = 0$  reached from the DVM<sup>21</sup> was indeed confirmed by the QMC in<sup>30</sup>. Possible supersolids were also studied in a  $d = 1$  lattice<sup>30</sup>. At  $d = 1$ , the SF to the CDW transition is in the Kosterlitz-Thouless (KT) transition universality class instead of the first order transition in  $d = 2$  and  $d = 3$ . We expect that the SF to the CDW-SS transition at  $d = 1$  is also in the KT transition universality class. The QMC simulations in a triangular lattice<sup>31</sup> found stable supersolids near  $1/3$  filling even for hard core bosons with  $U = \infty, V_1 > 0$ , as first predicted by the spin wave expansion in<sup>26</sup>. However, for hard core bosons with  $U = \infty, V_1 > 0$ , no stable supersolids were found near  $1/3$  fillings in a Kagome lattice<sup>32</sup>. But we do expect<sup>22,23</sup> that a CDW-VB supersolid should be stable in a soft core boson case with  $U < \infty, V_1 > 0$ . Furthermore, a stripe supersolid should be stable even in a hard core case with  $U = \infty, V_1 > 0, V_2 > 0$ .

### 3. QMC simulations in optical lattices with Dipolar bosons

Since the experimental realization of polar fermionic molecules<sup>33–40</sup>  $K + ^{87}Rb$ , there have been extensive research activities to study new states of matter which can be formed by these polar molecules<sup>34–36</sup>. Stable bosonic molecules  $^{39}K + ^{87}Rb$  should also be within experimental reach in the near future. The particular feature of these polar molecules are that they carry large electric dipole moments, therefore interact with each other via long-rang anisotropic dipole-dipole interactions similar to excitons in the EHBL in Sec.II-2. It was argued in Sect.II-2 that the dipole-dipole interaction between indirect excitons may favor a formation of vacancy-like exciton supersolid in some intermediate distances between the bilayers. Here, there are extensive numerical evidences that the dipole-dipole long-range interaction is especially favorable to the formation of the CDW supersolid<sup>34–36</sup>. Although the QMC simulations in<sup>27</sup> found that for hard-core bosons in a square lattice with the  $V_1 > 0$  interaction, the X-CDW is not stable against a phase separation slightly away from  $1/2$  filling, the QMC simulations in<sup>34</sup> found that for hard core bosons with the dipole-dipole interaction, the X-CDW is stable in a large parameter regime slightly away from  $1/2$  fillings. Furthermore, it was found the CDW-SS to the SF transition is a second order transition in the  $3d$  Ising universality class<sup>25</sup>, instead of a first order transition in the  $V_1 > 0$  case<sup>27</sup>. Very similarly, the  $\vec{Q}_n = 2\pi/3(1, 1)$  X-CDW supersolid were found to be stable in a large parameter regimes near the  $1/3$  filling in a triangular lattice<sup>35</sup>. Stable supersolid phase was also identified in dipolar bilayer systems<sup>36</sup>. In fact, the  $^{52}Cr$  atoms<sup>37</sup> carry exceptionally large magnetic dipole moment and therefore interact with each other also with the anisotropic long-range dipole-dipole interaction. All kinds of CDW and CDW supersolids could be very likely realized in near future experiments with either dipolar bosons or  $^{52}Cr$  atoms loaded in square and triangular lattices.

### 4. Detection of supersolids and their excitations in optical lattices

There could be many kinds of detection methods of possible supersolids in continuous systems such as the NCRI<sup>2,3</sup>, mass flow<sup>4,5</sup>, melting curve<sup>6</sup>, acoustic attenuation<sup>7</sup> and specific heat<sup>8</sup>. So far, the detection methods of the possible charge neutral cold atoms loaded in optical lattices are very limited. However, in recent works<sup>38,39</sup>, the authors developed a systematic and unified theory of using the optical Bragg scattering, atomic Bragg scattering or cavity QED to detect the ground state and the excitation spectrum of many quantum phases of interacting bosons loaded in bipartite and frustrated optical lattices. They showed that the two photon Raman transition processes in the three detection methods not only couple to the density order parameter, but also the *valence bond order* parameter due to the hopping of the bosons on the lattice. This valence bond order coupling is very sensitive to any

superfluid order or any Valence bond (VB) order in the quantum phases to be probed. These quantum phases include not only the well known superfluid and Mott insulating phases, but also other important phases such as various kinds of charge density waves (CDW), valence bond solids (VBS), CDW-VBS phases with both CDW and VBS orders unique to frustrated lattices, and also various kinds of supersolids. So if the supersolids of dipolar bosons or  $^{52}Cr$  atoms can indeed be realized in optical lattice, the light scattering methods discussed in<sup>38,39</sup> could be used to detect their existence and excitation spectra shown in Fig.2.

#### IV. SUPERFLUID DENSITY WAVE IN CONTINUOUS SYSTEMS

So far, we only discussed possible supersolids and their excitation spectra in bosonic systems. In fact, there is also an analog in fermionic systems which is the well known, but putative Larkin-Ovchinnikov-Fulde-Ferrell (LOFF) pairing state<sup>40,41</sup>. When the number of spin up electron is equal to the number of down spin electron  $n_\uparrow = n_\downarrow$ , then the pairing between them is at  $\vec{k} = 0$  only. If there is a mismatch  $\delta n = n_\uparrow - n_\downarrow$ , then pairing may shift to a non-zero momentum  $q_0 \sim k_{F\uparrow} - k_{F\downarrow}$  which is the FFLO pairing state. By using the GL theory near the transition from the normal to the FFLO state, at a mean field level, the authors in<sup>42</sup> constructed the GL free energy in the momentum space in terms of the S-wave pairing order parameter  $\psi_{FFLO}(\vec{x}) = \langle c_\uparrow^\dagger(\vec{x})c_\downarrow(\vec{x}) \rangle$ :

$$\begin{aligned} f = & \sum_G \frac{1}{2} r_G |\psi_G|^2 + u \sum_G \psi_{G_1} \psi_{G_2} \psi_{G_3} \psi_{G_4} \delta_{G_1+G_2+G_3+G_4} \\ & + v \sum_G \psi_{G_1} \psi_{G_2} \psi_{G_3} \psi_{G_4} \psi_{G_5} \psi_{G_6} \delta_{G_1+G_2+G_3+G_4+G_5+G_6} \end{aligned} \quad (9)$$

where  $r_G = T - T_c$  and  $u, v$  are the fourth and sixth order interaction terms respectively. This equation should be understood as an expansion in terms of the FFLO order parameter  $\psi_G$ , not as a gradient expansion anymore. The GL action was used to understand the lattice structure of the FFLO state. If  $r_G > 0$ , the system is in the normal state with  $\langle \psi(\vec{G}) \rangle = 0$ , while when  $r_G < 0$ , it is in the FFLO phase with the order parameter:  $\langle \psi(x) \rangle = \sum_{i=1}^P \Delta_i e^{i\vec{G}_i \cdot \vec{x}}$ ,  $|\vec{G}_i| = q_0$ . From Eqn.9, the authors found the most favorable lattice structures of the FFLO state is the stripe state (LO state with  $P = 2$ ) in large number of parameter regimes. The FFLO state maybe considered as a weak coupling (or fermionic) analog of the (bosonic) supersolid.

So far all the previous analysis in a FFLO state<sup>40-42</sup> are only at a mean field level. Just from symmetry breaking point of views, the FFLO state breaks both  $U(1)$  symmetry and the translational symmetry, therefore it also supports two kinds of Goldstone modes. (1) The Goldstone mode due to the  $U(1)$  symmetry breaking. (2) the lattice phonon modes due to the translational symmetry breaking. Above the mean field solution, very similar to the second equation in Eqn.1, the pairing order parameter can be written as:

$$\psi_{FFLO}(\vec{x}, \tau) = \Delta e^{i\theta(\vec{x}, \tau)} \sum_{\vec{G}}' e^{i\vec{G} \cdot (\vec{x} + \vec{u}(\vec{x}, \tau))} \quad (10)$$

where  $\theta(\vec{x}, \tau)$  and  $\vec{u}(\vec{x}, \tau)$  are the superfluid phonon and the lattice phonon modes respectively. The LO state corresponds to  $P = 2$ . For a charged condensed matter system such as

a electron system, due to the Higgs mechanism, the Goldstone mode  $\theta(\vec{x}, \tau)$  will be just eaten by the gauge field. However, for a neutral system such as the pairing between two species of fermions with unequal populations in cold atom systems across a Feshbach resonance, the Goldstone mode  $\theta(\vec{x}, \tau)$  survives. The coupling between the two phonon modes in Eqn.10 are also described by a equation similar to Eqn.3. The only difference is that the lattice structure is a LO state instead of an isotropic solid. After taking this difference into account, the elementary excitations inside the FF state are similar to those in the Fig.1b and the corresponding spectral weights can be worked out similarly. The experimental signatures of the elementary excitations can also be worked out similarly. Unfortunately, so far, there is still no convincing evidences for a FFLO state in either condensed matter or cold atom systems yet.

## V. SUPERFLUID DENSITY WAVE IN AN OPTICAL CAVITY

As shown in Sec.III, various kinds supersolids may be stabilized in the presence of long-range interactions. In this section, we discuss a superfluid density wave (SDW) of bosons where the long range interactions between bosons are mediated by cavity photons. The experimental set-up is shown in Fig.3a where cold atoms such as  $^{87}\text{Rb}$  are embedded in a high finesse standing wave cavity and are strongly interacting with cavity photons, subject to a transverse pumping. The probe detects the Florescence spectrum of small cavity leaking photons<sup>43,44</sup>. The mapping of the experimental set-up in Fig.3a to the  $Z_2$  Dicke model<sup>45</sup> Eqn.11 was given in<sup>44</sup>:

$$H_{Z_2} = \omega_c a^\dagger a + \frac{\omega_a}{2} \sum_{i=1}^N \sigma_i^z + \frac{g}{\sqrt{N}} \sum_{i=1}^N (a^\dagger + a)(\sigma_i^+ + \sigma_i^-) \quad (11)$$

In the frame rotating with the pumping frequency  $\omega_p$ , the two photon Raman process in the experimental set-up Fig.3a leads to:

$$\begin{aligned} H_{RS} = & \delta a^\dagger a + \int dx dz \Psi^\dagger(x, z) \left[ \frac{p_x^2 + p_z^2}{2m} + \frac{\Omega^2}{\Delta_a} \cos^2 kz \right. \\ & \left. + \frac{g_0 \Omega}{\Delta_a} (a^\dagger + a) \cos kx \cos kz + \frac{g_0^2}{\Delta_a} \cos^2 kx a^\dagger a \right] \Psi(x, z) \end{aligned} \quad (12)$$

where  $\delta = \omega_p - \omega_c$ ,  $\Delta_a = \omega_p - \omega_a$ . The  $Z_2$  symmetry is  $a \rightarrow -a$ ,  $kx \rightarrow kx + \pi$  or  $a \rightarrow -a$ ,  $kz \rightarrow kz + \pi$ .

At the mean field level, in the two modes approximation, one can decompose the atom field into the superpositions of two momentum (orbital) levels:

$$\Psi_{RS}(x, z) = c_0 \psi_0 + c_1 \cos kx \cos kz \psi_0 \quad (13)$$

where the  $\psi_0$  is the zero crystal momentum state of the lowest Bloch band of the one dimensional Hamiltonian  $H_{1d} = \frac{p_z^2}{2m} + \frac{\Omega^2}{\Delta_a} \cos^2 kz$  and  $c_0^\dagger c_0 + c_1^\dagger c_1 = N$ . Under the  $Z_2$  transformation,  $c_1 \rightarrow -c_1$ . When comparing Eqn.13 with Eqns.1,10, noting that  $\lambda_p = 2\pi/k$ ,  $\lambda = \lambda_p/2 = \pi/k$  in the Fig.3, one can see that the  $c_1$  term is just  $P = 4$  with  $\vec{G} = (\pm\pi, \pm\pi)$  which are the ordering wavevectors of a possible  $Z_2$  SFD.

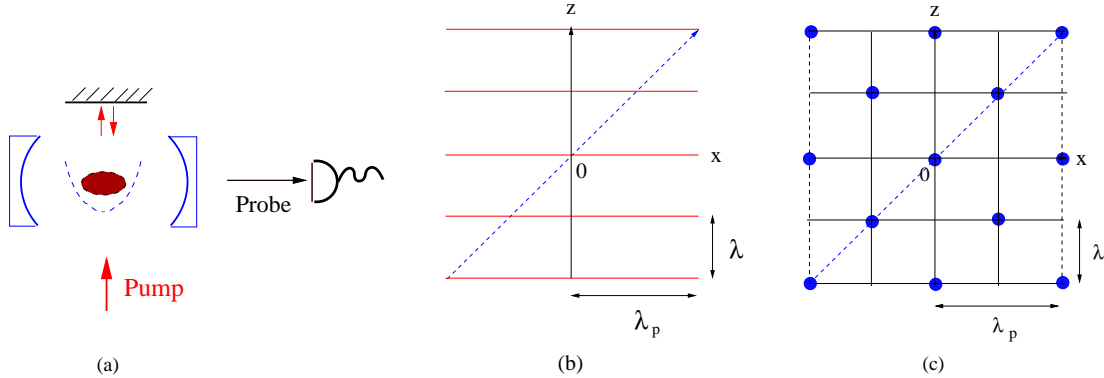


FIG. 3: (a) Reflected Transverse pumping plus the Standing wave cavity to realize the  $Z_2$  Dicke model, the probe detects the Florescence spectrum. The atom distributions of the  $Z_2$  Dicke model at  $N = \infty$ . (b) In the normal phase, the atoms just follow the stripes formed by the reflected transverse pumping. The  $\lambda_p = 2\pi/k$ ,  $\lambda = \lambda_p/2 = \pi/k$  where the  $k$  is the transverse pumping wave number (c) In the  $Z_2$  superradiant phase for photons and the  $Z_2$  supersolid state for atoms, the atoms take the check-board distribution on the optical lattice formed by the cavity photon and the pumping laser.

Substituting Eqn.13 into Eqn.12 leads to the interacting Hamiltonian between the photon and the effective two momentum ( orbital ) levels:

$$H_{J-Z_2} = \omega_c a^\dagger a + \omega_a J^z + \tilde{g}(a^\dagger + a)(J^- + J^+) \quad (14)$$

where  $\omega_c = \delta - N \frac{g_0^2}{2\Delta_a}$ ,  $\omega_a = 2\omega_r$  where  $\omega_r = \hbar^2 k^2 / 2m$  is the recoil energy. The effective interaction is  $\tilde{g} = \frac{g_0 \Omega}{\Delta_a}$  and  $J^z = \frac{1}{2}(c_1^\dagger c_1 - c_0^\dagger c_0)$ ,  $J^+ = c_0^\dagger c_1$ ,  $J^- = c_1^\dagger c_0$ . One can identify Eqn.14 with Eqn.11 after identifying the collective spin operators of the  $N$  atoms as  $J^z = \frac{1}{2} \sum_{i=1}^N \sigma_i^z$ ,  $J^+ = \sum_{i=1}^N \sigma_i^+$ ,  $J^- = \sum_{i=1}^N \sigma_i^-$ .

From Eqn.13, one can see the boson density:

$$n_{RS}(x, z) = \langle c_0^\dagger c_0 \rangle |\psi_0|^2 + \langle c_1^\dagger c_1 \rangle \cos^2 kx \cos^2 kz |\psi_0|^2 + \langle J^x \rangle \cos kx \cos kz |\psi_0|^2 \quad (15)$$

In the normal phase,  $\langle c_1^\dagger c_1 \rangle = 0$  and  $\langle J^x \rangle = 0$ , the boson density is just  $\sim |\psi_0|^2$  shown in Fig.3b. In the  $Z_2$  super-radiant phase,  $\langle c_1^\dagger c_1 \rangle > 0$  and  $\langle J^x \rangle \neq 0$ , the boson density takes the check-board pattern shown in Fig.3c. The corresponding SF to the SDW transition of the atoms is in the same universality class of the  $Z_2$  superradiance<sup>46</sup>.

Of course, any symmetry breaking only happens in the thermodynamic limit. For a finite system, the symmetry breaking will be restored. The quantum fluctuations ( namely, the finite size effects ) in the  $Z_2$  Dicke model is exponentially suppressed  $\sim e^{-N}$ , but still observable at small  $N$ . The quantum fluctuations will restore the  $Z_2$  symmetry, so render  $\langle J^x \rangle = 0$ , but still keep  $\langle c_1^\dagger c_1 \rangle > 0$  inside the  $Z_2$  super-radiant phase. They will transform the check-board pattern in Fig.3c to the uniform distribution on the optical lattice formed by the cavity photon and the pumping laser. The transition from the SF to the SDW becomes a crossover. The detailed study of quantum fluctuations were given in<sup>46</sup>.

## VI. CONCLUSIONS:

In this paper, we reviewed and also provided additional insights to possible supersolids and their excitation spectra in various systems. These systems could be continuous systems such as in 3d liquid Helium or 2d excitonic systems. The GL theory for such continuous systems were constructed in<sup>13-15</sup> and in<sup>18</sup>. It consists of two components: the normal solid component  $\delta n(\vec{x}) = n(\vec{x}) - n_0$  where the  $n_0$  is the average density and the superfluid component  $\psi(\vec{x})$  listed in Eqn.1. The  $\psi(\vec{x})$  stands for the quantum fluctuation generated vacancies or interstitials in an underlying in-commensurate solid whose condensation leads to the superfluid component inside the SS. At the mean field level, the GL theory can be used to understand the lattice structure of the supersolid which consists of a normal solid and also a superfluid density wave embedded inside such a normal lattice. It can also be used to study different classical and quantum transitions among the solid, liquid, superfluid and supersolid. Inside the SS phase, the effective action Eqn.3 controls the quantum fluctuations above the mean field lattice structure of  $\delta n(\vec{x})$  and the condensation structure of  $\psi(\vec{x})$ . From the effective action Eqn.3, we found that the elementary excitations have two longitudinal modes  $\omega_{\pm} = v_{\pm}q$  called "supersolidons" shown in Fig.1. The transverse modes in the SS stays the same as those in the NS. The effects of these two supersolidons on the in-elastic X-ray scattering, neutron scattering, acoustic attenuations and specific heat were discussed in<sup>13-15</sup>. So detecting these "supersolidons" by these experiments could be smoking gun experiments to confirm a supersolid in any continuous systems. We also argued that the dipole-dipole interaction in the in-direct excitons in 2d EHBL may favor the formation of a supersolid more than the Van der Waals interactions between <sup>4</sup>He atoms. Then we discussed the supersolids in lattice systems which are much simpler than its continuous counterpart. Much more solid theoretical results from spin wave analysis, dual GL and QMC are established in lattice supersolid cases. The dual GL theory in the dual vortex picture was developed from the magnetic space group in<sup>19-23</sup>. The dual GL theory be used to study different classical and quantum transitions among the CDW, VBS, CDW-SS, VB-SS superfluid and normal liquid transitions, also the excitation spectra in these quantum and classical phases. The elementary excitations in some of these phases were shown in the Fig.2 and can be contrasted to its continuous counterpart in the CDW case. There is no continuous counterpart in the VB case. Both interstitial or vacancy like supersolids can happen in lattices slightly away from 1/2 fillings in a bipartite lattice or 1/3 fillings in a frustrated lattice. So it can only happen at in-commensurate fillings. The SF flow inside the SS at these in-commensurate fillings are due to the interstitial or vacancies on top of the commensurate solid backbones. In this regard, the lattice supersolids are similar to its continuous counterparts. The CDW-SS could be realized in possible near future experiments with dipolar bosons or <sup>52</sup>Cr atoms loaded in various optical lattices.

We also discussed the superfluid density wave (SDW) in both fermionic and bosonic systems. The main difference than the supersolids is that the former only has one order parameter  $\psi(x)$  as shown in Eqn.10,13, no the underlying normal solid component  $\delta n(\vec{x}) = n(\vec{x}) - n_0$  shown in the first equation in Eqn.1. So the SDW can form at any density instead of just slightly away from commensurate fillings for a supersolid. The first example is the inhomogeneous superfluids ( FFLO state ) in a continuous system. Its excitation spectrum is also similar to those shown in Fig.1. So far, there is no clear experimental evidences of FFLO state in condensed matter or cold atom systems yet, but they are still under extensive searches in both communities. The second example is the  $Z_2$  SDW in an

optical lattice. Its excitation spectrum is also similar to those shown in Fig.2. There is clear experimental evidences of such  $Z_2$  SDW in cold atoms inside a transversely pumped high finesse cavity shown in Fig.3. We expect SDW may be realized in cold spinor atom BEC systems in the presence of strong spin-orbit coupling generated by artificial non-abelian gauge potentials<sup>47</sup>. The spin-orbit coupling may lead to spontaneous symmetry breaking of translational symmetry, then the theory presented in Sect.IV may apply to such a case. We expect theoretical investigations and experimental searches for various kinds of supersolids in various systems are still active underway.

### Acknowledgements

Y.C and Q.S.T's research are supported by NSFC-11074004. J. Ye thank A.V. Balatsky for his hospitality during J.Ye's visit at LANL. J. Ye's research is supported by NSF-DMR-1161497, NSFC-11074173, Beijing Municipal Commission of Education under grant No.PHR201107121, at KITP is supported in part by the NSF under grant No. PHY-0551164.

---

<sup>1</sup> A. Andreev and I. Lifshitz, Sov. Phys. JETP **29**, 1107 (1969); G. V. Chester, Phys. Rev. A **2**, 256 (1970); A. J. Leggett, Phys. Rev. Lett. **25**, 1543 (1970); W. M. Saslow , Phys. Rev. Lett. **36**, 1151-1154 (1976).

<sup>2</sup> E. Kim and M. H. W. Chan, Nature 427, 225 - 227 (15 Jan 2004), E. Kim and M. H. W. Chan, Science 24 September 2004; 305: 1941-1944, A. Clark and M. Chan, J. Low Temp. Phys. **138**, 853 (2005), E. Kim, M. H. W. Chan, Phys. Rev. Lett. **97**, 115302 (2006).

<sup>3</sup> Ann Sophie C. Rittner, John D. Reppy, Phys. Rev. Lett. **97**, 165301 (2006).

<sup>4</sup> James Day, T. Herman and John Beamish, Phys. Rev. Lett., vol 95, 035301 (2005).

<sup>5</sup> M. W. Ray and R. B. Hallock, Phys. Rev. Lett. 100, 235301 (2008); Phys. Rev. B 79, 224302 (2009).

<sup>6</sup> I. A. Todoshchenko, H. Alles, J. Bueno, H. J. Junes, A. Ya. Parshin, and V. Tsepelin, Phys. Rev. Lett. **97**, 165302 (2006); JETP **85**, 555 (2007).

<sup>7</sup> John M. Goodkind, Phys. Rev. Lett. **89**, 095301 (2002); G. Lengua and J. M. Goodkind, J. Low Temp. Phys. **79**, 251 (1990)

<sup>8</sup> C.A. Burns and J.M. Goodkind, J. Low Temp. Phys. **95**, 695 (1994).

<sup>9</sup> D. M. Ceperley, B. Bernu, Phys. Rev. Lett. **93**, 155303 (2004)

<sup>10</sup> D. E. Galli, M. Rossi, L. Reatto, Phys. Rev. B **71**, 140506(R) (2005).

<sup>11</sup> P. W. Anderson, W. F. Brinkman, David A. Huse, Science 18 Nov. 2005; **310**: 1164-1166.

<sup>12</sup> A. T. Dorsey, P. M. Goldbart, J. Toner, Phys. Rev. Lett. **96**, 055301 (2006).

<sup>13</sup> Jinwu Ye, Phys. Rev. Lett. **97**, 125302 (2006).

<sup>14</sup> Jinwu Ye, Europhysics Letters, **82** 16001 (2008)

<sup>15</sup> Jinwu Ye, J. Low Temp Phys. **160**(3), 71-111,(2010)

<sup>16</sup> P. Nozieres, J Low Temp Phys **156**, 9C21 (2009).

<sup>17</sup> C.-D. Yoo and Alan T. Dorsey, Phys. Rev. B **81**, 134518 (2010).

<sup>18</sup> Jinwu Ye, J. Low Temp Phys. **158**(5), 882-900 (2010).

<sup>19</sup> Balents L, *et al*, Phy. Rev. B **71**, 144508 (2005).

<sup>20</sup> Longhua Jiang and Jinwu Ye, J. Phys, Condensed Matter. **18** (2006) 6907-6922

<sup>21</sup> Jinwu Ye, Nucl. Phys.B **805** (3) 418-440 (2008).

<sup>22</sup> Yan Chen and Jinwu Ye, arXiv:0804.3429, v3, submitted to J. Phys. A.

<sup>23</sup> Yan Chen and Jinwu Ye, arXiv:0612009, v4, accepted for publication in Nucl. Phys. B.

<sup>24</sup> Anders W. Sandvik, Phys. Rev. Lett. 98, 227202 (2007).

<sup>25</sup> One can understand these results from Fig.2 intuitively. (1) From Right to the middle in Fig.2. Across the transition from the CDW ( VBS ) to the CDW-SS ( VB-SS), the SF mode is the only low energy mode, the CDW (VBS) mode has a gap across the transition, so non-critical and can be integrated out, so the CDW to the CDW-SS transition is in the same universality class of the Mott to SF transition. (2) From left to the middle in Fig.2. Across the transition from the  $SF_1$  (  $SF_2$  ) to the CDW-SS ( VB-SS), there are SF modes on both side, so it may couple to possible critical density fluctuation mode ( if it exists at a 2nd order transition ), so the nature of the transition is much more complicated, may be resolved by high precision QMC on specific microscopic models. For example, the  $V_1 > 0, V_2 > 0$  model Eqn.8 may be in a different universality class than the dipole-dipole intercation model.

<sup>26</sup> G. Murthy, D. Arovas, A. Auerbach , Phys. Rev. B 55, 3104-3121 (1997).

<sup>27</sup> F. Hebert *et.al*, Phys. Rev. B 65, 014513 (2001)

<sup>28</sup> P. Sengupta, *et.al*, Phys. Rev. Lett. 94, 207202 (2005).

<sup>29</sup> Jing Yu Gan, Yu Chuan Wen, Jinwu Ye, Tao Li, Shi-Jie Yang, Yue Yu, Phys. Rev. B 75, 214509 (2007).

<sup>30</sup> G.G. Batrouni, *et.al* Phys. Rev. Lett. 97, 087209 (2006), Phys Rev A72, 031601(R) (2005).

<sup>31</sup> D. Heidarian and K. Damle, Phys. Rev. Lett. **95**, 127206 (2005); S. Wessel and M. Troyer, Phys. Rev. Lett. **95**, 127205 (2005).

<sup>32</sup> S. V. Isakov, *et al*, Phys. Rev. Lett. 97, 147202 (2006); Kedar Damle, T. Senthil, Phys. Rev. Lett. 97, 067202 (2006).

<sup>33</sup> K.-K. Ni, *et al*, Science 322, 231 (2008).

<sup>34</sup> B. Capogrosso-Sansone, *et al*, Phys. Rev. Lett. 104, 125301 (2010). It seems there is a factor of  $1/N$  missing in the structure factor defined in this paper.

<sup>35</sup> L. Pollet, J. D. Picon, H. P. Bkhler, and M. Troyer, Phys. Rev. Lett. 104, 125302 (2010).

<sup>36</sup> J. R. Armstrong, N. T. Zinner, D. V. Fedorov and A. S. Jensen, EPL 91 16001 (2010).

<sup>37</sup> A. Griesmaier, *et.al*, Phys. Rev. Lett. 94, 160401 (2005)

<sup>38</sup> Jinwu Ye, J.M. Zhang, W.M. Liu, K.Y. Zhang, Yan Li, W.P. Zhang, Phys. Rev. A 83, 051604 (R) (2011).

<sup>39</sup> Jinwu Ye, J.M. Zhang, W.M. Liu, K.Y. Zhang, Yan Li, W.P. Zhang, Yan Chan and CunLin Zhang, arXiv:0812.4077, v5, submitted to Phys. Rev. A.

<sup>40</sup> P. Fulde and R. A. Ferrell, Phys. Rev. 135, A550?A563 (1964).

<sup>41</sup> A. I. Larkin and Yu. N. Ovchinnikov, Sov. Phys. JETP 20, 762(1965)

<sup>42</sup> Longhua Jiang and Jinwu Ye, Phys. Rev. B 76, 184104 (2007).

<sup>43</sup> A. T. Black, H. W. Chan and V. Vuletic, Phys. Rev. Lett. 91, 203001(2003).

<sup>44</sup> K. Baumann, *et.al*, Nature 464, 1301-1306 (2010).

<sup>45</sup> For  $U(1)$  and  $Z_2$  Dicke models, see Jinwu Ye and CunLin Zhang, Phys. Rev. A 84, 023840 (2011).

<sup>46</sup> Yu Chen, Jinwu Ye and Quang Shan Tian, preprint.

<sup>47</sup> Jean Dalibard, Fabrice Gerbier, Gediminas Juzelinas, Patrik Ohberg, arXiv:1008.5378. To appear in Rev. of Mod. Phys.